

## ESDA2010-25069

### NUMERICAL APPROACH TO DESIGN PROCESS OF ARMORED VEHICLES

**Atil Erdik\*, Namik Kilic**

Otokar Otomotiv ve Savunma Sanayi A.S,  
CAE Department, Sakarya, Turkey

**Prof. Mustafa Guden, Ass.Prof. Alper  
Tasdemirci**

Izmir Institute of Technology, Department of  
Mechanical Engineering, İzmir, Turkey

#### ABSTRACT

Today, it is imperative that armored vehicles need advanced protection kits against anti-symmetric threats more than before. The primary goal of this study was to assess benefits of explicit hydrocodes for mine protection resistance of armored vehicles. An analysis of an armored vehicle under blast loading caused by high explosive (HE) detonation is presented with comparison to a full-scale test. The problem was examined using LS-DYNA which is an explicit non-linear finite element code. Multi Material Arbitrary Lagrangian Eulerian (MM-ALE) Fluid Structure Interaction Method was selected to model the explosion domain so as to observe advancing of the shock wave in the compressed air and to investigate the effects of blast on the vehicle structure after explosion. Johnson-Cook constitutive material model, Jones-Wilkins-Lee (JWL) and Linear Polynomial equation of states were used for the problem. Results show that numerical analysis was in good agreement with the experimental result.

#### INTRODUCTION

In modern world, asymmetric threats severely affect military vehicles and their occupants. Numerical simulations can be useful to estimate blast damage on vehicle body and to improve durability of vehicles against mine blast attacks.

The assessment of blast loading and damage on structures and equipment is crucial in a wide range of military applications. During design process of military vehicle, prototypes are built and used in destructive field-tests in order to determine the level of blast resistance of the vehicle. The field test is not only time consuming, but also costly and it might not ensure an optimized design. In addition, a variety of field conditions and other related factors make each blast test difficult to perform.

Simulation capability is important to accurately interpret the blast loading and structural response. Recent advances in commercially available finite element codes have made

numerical methodologies suitable for simulations of coupled blast-structural response. The non-linear finite element code, LS-DYNA [1], has Arbitrary Lagrangian-Eulerian (ALE) method coupled with classical Lagrangian structural analysis methods allow a fully coupled approach to solve blast-structure interactions.

#### MINE BLAST SIMULATION

Computer codes have matured considerably since their initial development. They now serve as valuable design tools in studies of materials and structures which are heavily subjected to intense impulsive loading at high strain rates [2].

#### Defining Of Simulation Methodology

Engineering models describing pressure histories due to explosions have been used for design purposes for many years. To illustrate this, the United States Army technical manual "Fundamentals of Protective Design for Conventional Weapons" written in 1986, is often cited as such a source document. This document also served as the basis for a popular software implementation known as CONWEP (CONventional WeaPons). Randers-Pehrson and Bannister (1997) implemented the air blast section of CONWEP into DYNA2D & DYNA3D. \*LOAD\_BLAST keyword activates CONWEP model in LS-DYNA [3-4]. This method is based on applying a previously known function of loading (Pressure segments) to the structure. The time space characteristics of pressure loads can be defined on the basis of data collected in a series of experiments. Despite its simplicity, this method of analysis of the structure behavior under blast loading leads to serious limitations. First, no interaction between the structure response and the acting force (Blast wave) is included. Simultaneous modeling and interaction between blast wave and structure is now possible by inserting the methodology, Arbitrary Lagrangian-Eulerian (ALE) coupling, which is implemented into LS-DYNA. After the addition of the ALE solver to LS-DYNA, a more general

\*Corresponding author, e-mail address: aerdik@otokar.com.tr

and powerful blast loading simulation capability was made available to the user community. The ALE capability allows for explicitly modeling both the blast media (air, water, solid) and the explosive. For this reason, ALE method was selected to perform blast simulations in this study.

The HE detonation and the process of shock propagation in the air were modeled using the mesh with the Euler's formulation. Structure was modeled using the mesh with the Lagrange's formulation. These two formulation were combined by activating \*CONSTRAINED\_LAGRANGE\_IN\_SOLID keyword in LS-DYNA. After coupling, Lagrangian models of structures were easily be inserted into the ALE mesh.

The model chiefly consists of three sections:

1. High Explosive (Eulerian Model)
2. Air Domain (Eulerian Model)
3. Structure (Lagrangian Model)

### High Explosive

NATO STANAG 4569 have described test conditions for NATO member countries to determine the protection level of logistic and light armored vehicles subjected to grenade and blast mine threats.

Field test is conducted with two ways depend on mine position. The mine can be either buried in soil or put into steel pot in accordance with NATO STANAG 4569 [3]. In order to reduce uncertainty during validation period of numerical simulations, in this study mine was planted into a steel pot. Furthermore using steel pot increases repeatability of tests and reliability of numerical analyses.

The high explosive is ignited at the center of mine using material \*MAT\_HIGH\_EXPLOSIVE\_BURN, can be seen in Table 1. In this model, the ignition time of a particle in the high explosive is equal to its distance to the ignition point divided by the detonation velocity [6].

**Table 1.** Material data of TNT

Density	1630 kg/m <sup>3</sup>
Detonation velocity	6930 m/s
Chapman-Jouget pressure	21.0 GPa
Internal energy density (E0)	7.0 GPa

### Equation of State Of High Explosive

The evaluation of the explosive after ignition was described by the Jones-Wilkins-Lee (JWL) equation of state, defined as \*EOS\_JWL in LS-DYNA.

The JWL equation of state defines pressure as a function of relative volume,  $V$ , and internal energy per initial volume,  $E$ , as

$$p = A \left[ 1 - \frac{w}{R_1 V} \right] e^{-R_1 V} + B \left[ 1 - \frac{w}{R_2 V} \right] e^{-R_2 V} + \frac{wE}{V} \quad (1)$$

Where  $w, A, B, R_1$  and  $R_2$  are user defined input parameters. The JWL equation of state was used to determine

the pressure of detonation products of high explosives in applications including metal accelerations. Input parameters for this equation are given by Dobratz (1981) for a variety of high explosive materials (Table 2) [6-7].

**Table 2.** Material constants of the JWL EOS for TNT

$w$	0.30
A	371.213 GPa
B	3.2306 GPa
$R_1$	4.15
$R_2$	0.95

### Air Domain

Air domain also called FSI calculation domain, encloses high explosive and structure. The air volume was meshed with brick elements. Material data for air is given in Table 3.

**Table 3.** Material data of Air

Initial density, $\rho_0$	1.293 kg/m <sup>3</sup>
Initial pressure	1 Bar
Ratio of specific heats, $\gamma$	1.4

### Equation of State Of Air

The air was described as an ideal gas. The expansion of the blast wave is assumed an adiabatic process. The \*MAT\_NULL material and \*EOS\_LINEAR\_POLYNOMIAL equation of state in LS-DYNA were used to express the constitutive relation below;

This polynomial equation of state, linear in the internal energy per initial volume,  $E$ , is given by:

$$p = C_0 + C_1 \mu + C_2 \mu^2 + C_3 \mu^3 + (C_4 + C_5 \mu + C_6 \mu^2) E \quad (2)$$

Here,  $C_0, C_1, C_2, C_3, C_4, C_5$  and  $C_6$  are user defined constants and

$$\mu = \frac{1}{V} - 1 \quad (3)$$

Where  $V$  is the relative volume. In expanded elements, the coefficients of  $\mu^2$  are set to zero, i.e.,

$$C_2 = C_6 = 0 \quad (4)$$

The linear polynomial equation of state might be used to model gas with the gamma law equation of state. This is achieved by setting:

$$C_0 = C_1 = C_2 = C_3 = C_6 = 0 \quad (5)$$

And

$$C_4 = C_5 = \gamma - 1 \quad (6)$$

Where  $\gamma$  is the ratio of specific heat. The pressure is then given by:

$$p = (\gamma - 1) \frac{\rho}{\rho_0} - 1 \quad (7)$$

## Johnson-Cook Material Model

Computational results are directly related to the quality of the material model in the code - the better the description of material behavior at the strain rates researcher interested in and of its fracture behavior at those strain rates- the better the computational results. Improper material characterization leads not only to quantitatively incorrect results but frequently to descriptions that are qualitatively incorrect. Imperfect understanding of this situation frequently leads to an undesirable iterative procedure of matching imperfectly understood experiments with theoretical computations based on incomplete models [2].

Johnson-Cook constitutive material model (1983) primarily intended for computations. It is recognized that more complicated models may indeed give more accurate descriptions of material behavior. Similarly, various models may give better descriptions for various materials. In many cases, however, the computational user cannot readily incorporate complicated and diverse models. The result is that a constant "dynamic flow stress" is often used [8].

Moreover, it is not based on traditional plasticity theory that reproduces several important material responses observed in impact and penetration of metals. The three key material responses are strain hardening, strain-rate effects, and thermal softening. These three effects are combined, in a multiplicative manner, in the Johnson-Cook constitutive model:

$$\sigma_Y = \left[ A + B \left( \varepsilon_{eff}^P \right)^N \right] \left[ 1 + C \ln \dot{\varepsilon} \right] \left[ 1 - (T_H)^M \right] \quad (8)$$

$\varepsilon_{eff}^P$  = effective plastic strain

$\dot{\varepsilon} = \frac{\varepsilon_{eff}}{\varepsilon_0}$  Where  $\dot{\varepsilon}_0$  is strain rate used to determine  $A$ ,  $B$

and  $N$ .

$T_H = \frac{T_R}{T_M - T_R}$  Is Homologous Temperature

$T_M$  = melting temperature

$T_R$  = reference temperature when determining  $A$ ,  $B$  and  $N$ .

Where the first bracketed term represents the strain hardening of the yield stress, the next term models the increase in the yield stress at elevated strain rates, and the final bracketed term is a softening of the yield stress due to local thermal effects.

The above yield strength portion of the Johnson-Cook constitutive model has five parameters:  $A$ ,  $B$ ,  $N$ ,  $C$  and  $M$ , and three material characteristics:  $\rho$ ,  $C_P$ , and  $T_M$ . Additionally, the elastic parameters are required. Typically the shear modulus is input along with an Equation-of-State (EOS) used to define the pressure versus volume strain response; for low pressures, the EOS is assumed to be defined by the elastic bulk modulus.

## Damage Factor on the J-C Model

Johnson and Cook (1985) expanded on their basic model with the inclusion of a model for fracture based on cumulative-damage; the LS-DYNA implementation of the JC constitutive model includes this additional model feature. The cumulative-damage fracture model;

$$\varepsilon^F = \left( D_1 + D_2 \exp \left[ D_3 \frac{P}{\sigma_{eff}} \right] (1 + D_4 \ln \dot{\varepsilon}) (1 + D_5 + T_H) \right) \quad (9)$$

Where  $D_i$ ,  $i=1, \dots, 5$  are input constants.

$$D = \sum \frac{\Delta \varepsilon_{eff}^P}{\varepsilon^F} \text{ Failure occurs when } D=1$$

Where

$\sigma_{eff}$  : Effective stress

$P$  : Mean stress (Pressure)

Is similar in form to the yield strength model with three bracketed regions combined in a multiplicative manner to include the effect of stress triaxiality, strain rate, and heating, respectively [7].

## Determination of the J-C Parameters

Conventional mechanical test systems have been available for years to obtain strength data under long term conditions (hours to days) or static conditions (minutes) using screw or hydraulic loading systems. The maximum deformation or strain rate of these machines is about 0.1 per second ( $0.1s^{-1}$ ). Pendulum impact machines such as Charpy or Izod can produce strain rates of up to about  $100s^{-1}$ , yielding only energy absorbed to fracture, but not a complete stress-strain curve. However, SHPB fills the strain rate range from  $10^2s^{-1}$  to  $5.0 \cdot 10^3s^{-1}$ , the time duration of many explosive, ballistic impact, crashes and other accident scenarios of interest for both military and civilian applications [9].

Four different types of tensile tests are required to identify the material constants used in the model. Quasi-static tensile tests are used to identify the elastic constants  $E$  and  $\nu$ , and  $A$ , the yield stress of the material. Notched-specimen tensile tests are used to define the strain hardening constants  $B$  and  $n$ , the fracture strain constants  $D_1$ ,  $D_2$ , and  $D_3$ . Dynamic tensile tests give the viscoplastic constant  $C$  and the fracture strain constant  $D_4$ . Tensile tests at elevated temperatures provide the constants  $m$ , and  $D_5$ , defining the temperature effect on the stress-strain curve and on the fracture strain, respectively.

For determining J-C material model and damage parameters of armor steel used in simulations, Dynamic Test & Modeling Laboratory at Izmir Institute of Technology (IYTE) performed numerous experiments.

## Quasi-static Tensile Tests

Several specimens were tested at various deformation rates, 0.15mm/min, 1.5mm/min, 15mm/min, and 150mm/min.

**Table 4.** Static test specifications

Deformation Rate (mm/min)	Nominal Test Rate (1/s)	Gage Length (mm)
0,15	0.0001	10 and 25
1,5	0.001	10 and 25
15	0.01	10 and 25
150	0.1	10 and 25

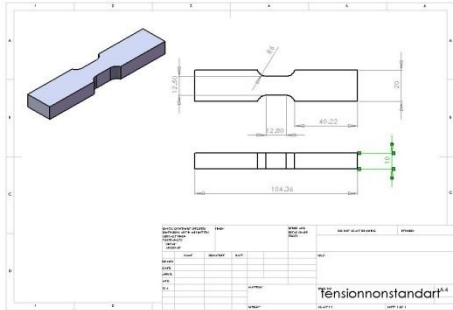
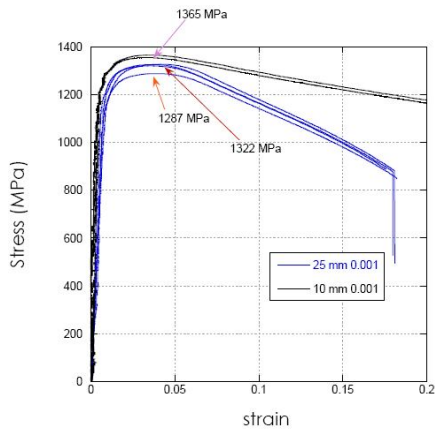


**Figure 1.** Dimensions of specimens used in quasi-static tensile test

True stress - true strain curves are shown in Figure 2. Quasi-static tensile test apparatus and specimen used in test can also seen in Figure 2.b, 2.c, and 2.d, respectively.



(a)



(b)



(c)



(d)

**Figure 2.** (a) True stress-true strain curves, at 0.001/s deformation rates, (b) - (c) Static test apparatus (d) Specimen

### Dynamic Split-Hopkinson Pressure Bar Tests

Dynamic material tests were carried out using Split-Hopkinson Pressure Bar (SHPB) apparatus at Dynamic Test and Modeling Laboratory at IYTE. SHPB is a mechanical test instrument which was used to characterize the dynamic response of materials at high strain rates (Figure 3) [10].



**Figure 3.** Split-Hopkinson Pressure Bar apparatus

A Gas gun launches a striker bar impacts on the end of the incident bar. A stress wave generated travels down the bar and is recorded sequentially by the first and second strain gages

mounted longitudinally on the bar. The stress wave then passes through the specimen and then the specimen is compressed. Part of the stress wave is reflected in the form of a tensile pulse and the remainder is transmitted to the transmitter bar and recorded by the third strain gage mounted on the transmitter bar. The three readings are used to determine the time dependent stress state of the specimen. From the time dependent strain data, a stress vs. strain plot can be obtained [3-10].

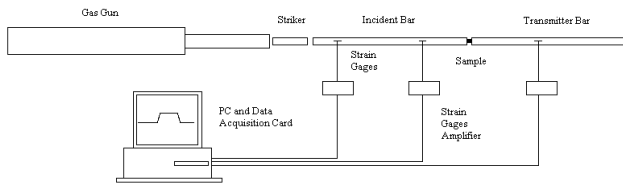


Figure 4. A Schematic representation of the SHPB

Voltage-stress conversion formula gives stress values of dynamic test:

$$\sigma = 2C_0V \cdot 10^6 \times \frac{2}{(Gain) \cdot (f)(1+\nu)(Ec)} \times 1000 / L_0 \quad (10)$$

Where

- $\sigma$  : Stress
- $C_0$  : Wave speed
- $V$  : Voltage values
- $Gain$  : Gains of amplicator
- $f$  : Factor of strain gage
- $\nu$  : Poisson ratio
- $E_c$  : Stress bridge voltage
- $L_0$  : Initial lengths

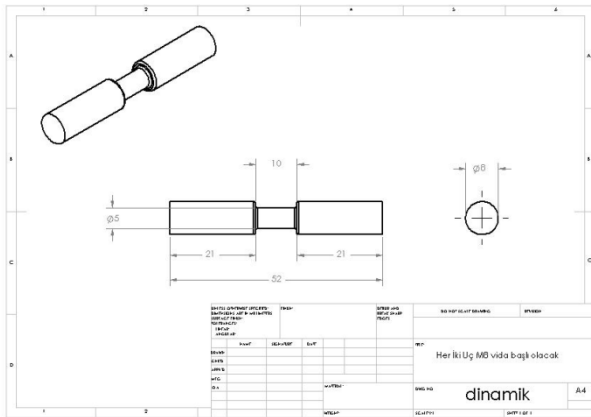


Figure 5. Dimensions of dynamic test specimens

Specimens with the span of 10mm. and 15mm. length and with 4mm and 3mm. diameter were tested at high strain rates (Figure 5). Dynamic test data and specimen used in Split-Hopkinson test can be seen in Figure 6.a and 6.b, respectively.

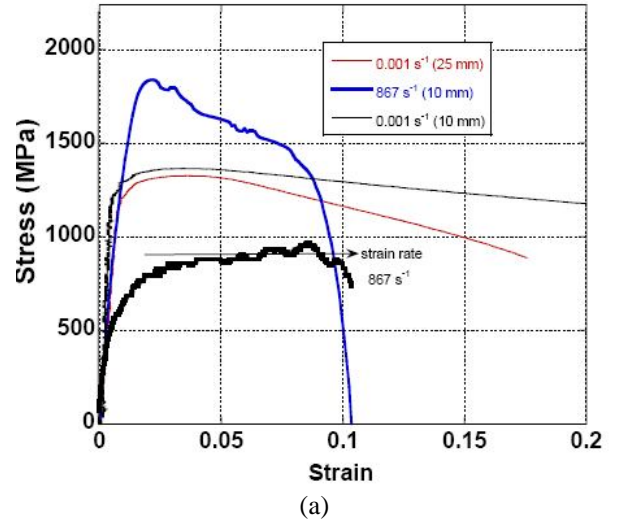


Figure 6. (a) Dynamic test data, (b) Specimen

### FEA MODEL OF ARMORED VEHICLE

Verification period of FEA model with field test not only takes time and a great deal of engineering effort, but also increases prototyping cost. Sometimes, only one part or just a specific section of the body is used in tests. We kept same methodology in this study. For this reason underneath of the vehicle and small amount of HE were modeled for the blast test (Figure 7). From this point on, all of these sections of the vehicle prepared for test is called as "fixture".

The fixture consists of several parts including supporting legs, supporting beams, the hull, a sandwich structure, and a few structural components from the lower section of the vehicle (Figure 8) [11].



Figure 7. Fixture used in the test

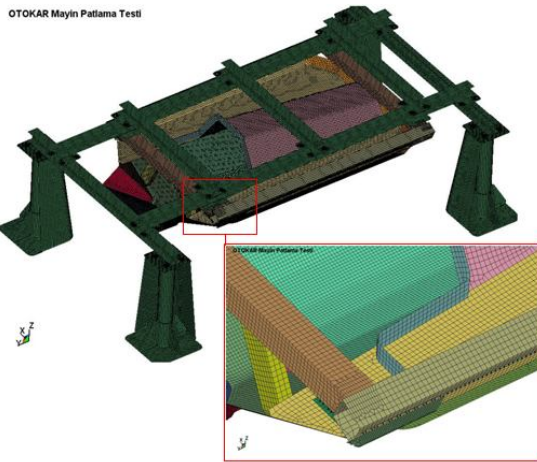


Figure 8. FEA model of Fixture

Belytscho-Tsay shell elements with two integration points were selected as Lagrangian elements. ALE solid elements were chosen for air domain, steel pot, and HE. Modeling details can be seen in Table 6. Hull is made from armor steel, and the other parts are made from mild steel. \*MAT\_JOHNSON\_COOK material model was defined for the structural parts. \*MAT\_PLASTIC\_KINEMATIC\_TITLE was used for steel pot (Fig.9). \*MAT\_NULL was used for Air domain. Mechanical properties of materials which are used in simulation are listed in Table 7 [12-13].

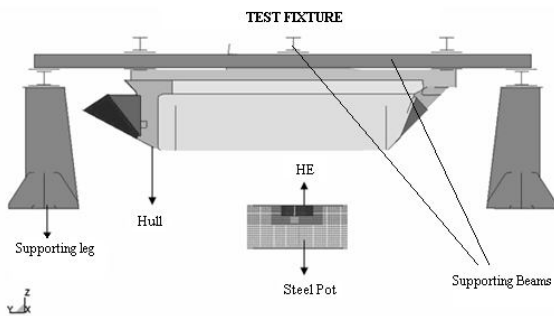


Figure 9. FEA model of fixture

Table 6. Modeling Details

Total number of nodes	715353
Total number of elements	691897
Element Types	
Shell Elements	223989
Solid Elements (Air, HE, Steel Pot, Bolts)	467908
Total Rigid Elements	55591
Total Deformable Elements	636306
Spot welds	924

Table 7. Material Properties

Material	LS-DYNA Cards (cm, g, us, 10MN)			
	*MAT_JOHNSON_COOK_TITLE			
	RO	E	PR	Fracture (D1)
Aluminum	2,66	0,70	0,33	0,5
Armor steel	7,86	2,06	0,30	0,3
Mild steel	7,86	2,10	0,30	0,4
	*MAT_PLASTIC_KINEMATIC_TITLE			
	RO	E	PR	Failure Strain
Steel Pot	7,86	2,06	0,30	0,5

## RESULTS

Energy data of simulation can be helpful to understand the behavior of the blast phenomenon. In other words, energy should be conserved at any time of the explosion. Elastic strain values and external work can be determined by investigating internal energy of the system. During the wave propagation, plastic deformation in the structure emerges while internal energy bursts out. As it can be seen in Figure 10, at the time of  $t=0$  HE detonates. As shock waves hit V-hull at the time of 200  $\mu$ s, pressure reaches V-hull and deflects it upward. Then V-hull interacts with the structure and move together while elastic deformation value on the V-hull reaches its peak point. At the beginning from 4400  $\mu$ s, deformation dramatically slows down and it subsequently comes at its final position [11].

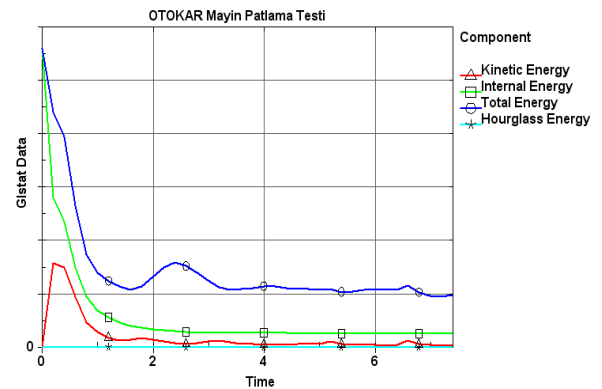
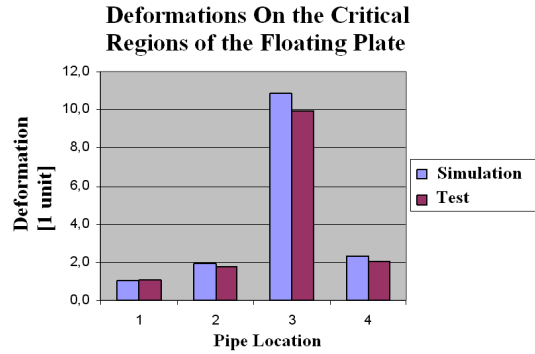


Figure 10. Energy balance of the system

As it can be seen in Figure 11, simulation results are close to those of field test.



**Figure 11.** Comparison between field test and simulation

In Figure 12 and Figure 13, deformation pattern and amounts show that simulation fits well with the test results [11].



**Figure 12.** Stress concentration on the V-hull



**Figure 13.** Field test results

## CONCLUDING REMARKS

In defense industry researches, protecting vehicles and occupants against landmines and asymmetric threats, and improving protection levels of vehicles occupy too much working time and cost. Both experiments and numerical analyses are crucial to design steps. Once simulations are validated with tests, FEA model can be used as a design tool throughout the development process. Analysis results help us not only to reduce time and cost, but also to understand experimental results.

## ACKNOWLEDGEMENTS

The authors wish to acknowledge Otokar Otomotiv ve Savunma Sanayi A.S. staffs who participate in this exhausting labor from field tests to simulations as crew members.

## REFERENCES

- [1] Hallquist, J.O., *LS-DYNA Keyword User's Manual Vol-I*, Livermore Software Technology Corporation, California, USA, 2007.
- [2] Zukas, J.A., Nicholas, T., Swift, H.F., Greszczuk, L.B., Curran, D.R., *Impact Dynamics*, New York, USA, 1982, pp 369-370.
- [3] Grujicic, M. et al., 'Computer-Simulations Based Development of A High Strain-Rate, Large-Deformation, High-Pressure Material Model for STANAG 4569 sandy gravel', *Soil Dynamics and Earthquake Engineering*, 2007, pp. 2-3.
- [4] Le Blanc, G., Adoum, M., Lapoujade, V., 'External Blast Load on Structures', *5th European LS-DYNA Users Conference*, Birmingham, UK, 2005, pp. 6-7.
- [5] Nato Army Armaments Group, 'Protection Levels for Occupants of Logistics and Light Armored Vehicles', *STANAG 4569*, NATO, 1999.
- [6] Alia, A., Souli, M., 'High Explosive Simulation Using Multi-Material Formulations', *Applied Thermal Engineering*, 2005.
- [7] Hallquist, J.O., *LS-DYNA Theory Manual*, Livermore Software Technology Corporation, California, USA, 2006.
- [8] Johnson, G.R., Cook, W.H., 'A Constitutive Model and Data for Metals Subjected To Large Strains, High Strain Rates and High Temperatures', *Proceedings of the 7th International Symposium on Ballistics*, The Hague, the Netherlands, 1983.
- [9] 'An Historic Mechanical Engineering Landmark', *Split Hopkinson Pressure Bar Apparatus*, Designation Ceremony, Southwest Research Institute, Texas, USA, 2006.
- [10] Dynamic Test and Modeling Laboratory, *Otokar Technical Report*, Izmir Institute of Technology, Izmir, Turkey, 2008, pp 6-11.
- [11] Erdik, A., Kilic, N., Kibaroglu, K., 'Improving the Protection Level of Light-Weight Armored Vehicles Against Landmines By Using Numerical Simulation Techniques', *SAVTEK 2008*, Ankara, Turkey, 2008, pp. 65-73.
- [12] Wang, J., 'Simulation of Landmine Explosion Using LS-DYNA3D Software', *DSTO-TR-1168*, DSTO Research Laboratory, Fisherman Bend, Australia, 2001, pp. 12-13.
- [13] Mullin, M.J., O'Toole, B.J., 'Simulation of Energy Absorbing Materials in Blast Loaded Structures', *8th International LS-DYNA Users Conference*, Detroit, USA, 2004, pp. 2-7.